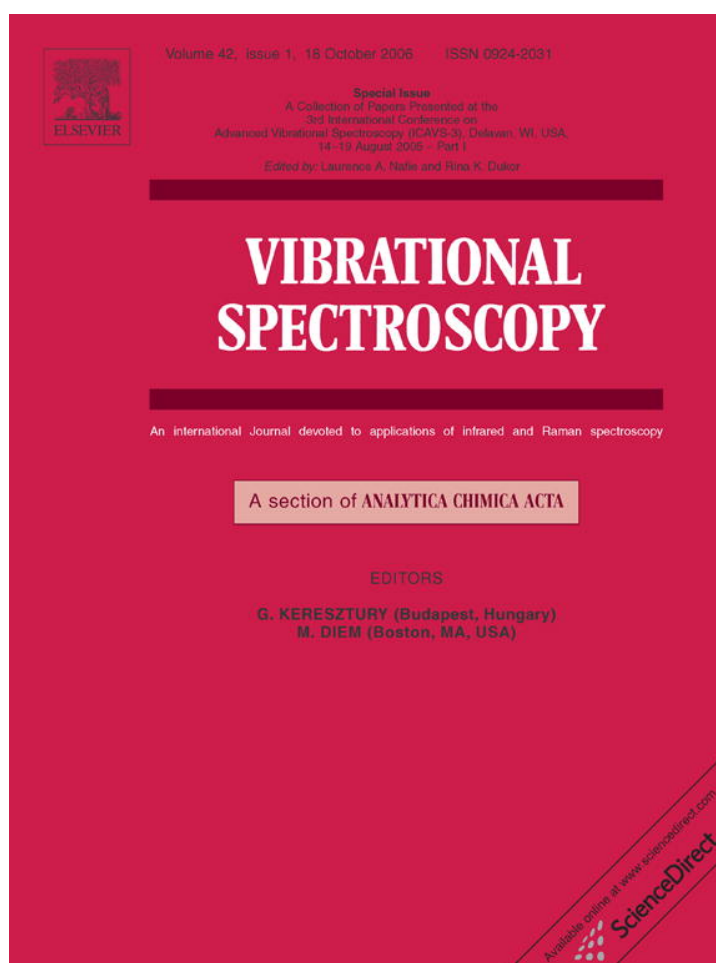


Provided for non-commercial research and educational use only.
Not for reproduction or distribution or commercial use.



This article was originally published in a journal published by Elsevier, and the attached copy is provided by Elsevier for the author's benefit and for the benefit of the author's institution, for non-commercial research and educational use including without limitation use in instruction at your institution, sending it to specific colleagues that you know, and providing a copy to your institution's administrator.

All other uses, reproduction and distribution, including without limitation commercial reprints, selling or licensing copies or access, or posting on open internet sites, your personal or institution's website or repository, are prohibited. For exceptions, permission may be sought for such use through Elsevier's permissions site at:

<http://www.elsevier.com/locate/permissionusematerial>



Contribution of transition dipole coupling to amide coupling in IR spectra of peptide secondary structures

Jan Kubelka^{a,b}, Joohyun Kim^a, Petr Bour^c, Timothy A. Keiderling^{a,*}

^a Department of Chemistry, University of Illinois at Chicago, 845 W. Taylor St. (m/c 111), Chicago, IL 60607-7061, United States

^b Department of Chemistry, University of Wyoming, Laramie, WY 82071, United States

^c Institute of Organic Chemistry and Biochemistry, Academy of Science, Flemingovo nam. 2, 16610 Prague 6, Czech Republic

Available online 23 May 2006

Abstract

Transition dipole coupling (TDC) is often regarded as a principal mechanism for vibrational coupling that is the basis for the conformational sensitivity of amide vibrations in peptides and proteins. We have computationally tested the relative contribution of TDC to coupling of amide I bands in model peptides. First, the amide I IR spectra were calculated for sizable peptides (up to 12 amides) in both α -helical and β -sheet conformations at the density functional theory (DFT) level. Second, the spectra were calculated using TDC to approximate long-range vibrational coupling between the local (diagonal) vibrational parameters, which were transferred from DFT calculations on smaller fragments. The TDC contribution was obtained using classical representations, but employed DFT-determined transition dipole moments of the fragments. Full DFT simulations of the peptide vibrational spectra have greater dispersion than those obtained by TDC corrections, which reflects an underestimate of amide coupling in the TDC, although this difference does decrease at long distances. If DFT computations are used for in-strand coupling, then TDC does give reasonable interstrand coupling magnitudes for β -sheet models. These systematic analyses show that TDC alone cannot account for the vibrational interactions that give rise to the characteristic amide I band-shapes.

© 2006 Elsevier B.V. All rights reserved.

Keywords: Peptide amide I IR; α -Helix; β -Sheet; Transition dipole coupling; Density functional theory

1. Introduction

The past decade has seen a large growth in the use of vibrational spectroscopic techniques to determine secondary structure in proteins and peptides [1,2]. Although IR spectroscopy has been long a tool of peptide and protein chemists, the development of Fourier transform IR (FT-IR) instruments with exceptional signal to noise ratio and of computational methods to enhance apparent resolution in measured spectra of heterogeneous structures has stimulated its broader use for structural questions. Similarly, continued advances in Raman spectroscopy, including resonance Raman effects, have had similar impact [3–7]. The basis of the sensitivity of the vibrational spectroscopies to polypeptide secondary structure arises from coupling between the amide vibrational modes which is sensitive to the peptide backbone conformation (ϕ , ψ

torsional angles) as well as to the hydrogen bonding. Recent developments in femtosecond laser-based 2D IR methods [8–10,11,12,13], site specifically isotope-labeled structure-spectra studies [14–17,18,19,20,21], vibrational circular dichroism (VCD) [22–25] and coupled IR, Raman and VCD studies [3,4,26] have emphasized the need to establish reliable understanding of the structural basis for vibrational coupling between amides.

Vibrational coupling of sequential amide groups in a polypeptide chain involves the interaction of vibrating atoms through the electronic structure (bonds). In a classical picture, such through-bond coupling can be viewed as “mechanical” (in the harmonic approximation, literally, as a spring). However, the basis of longer distance coupling is much less obvious, and might be largely dominated by electrostatic effects, with dipolar coupling being the leading term. The latter approximation has been the basis for several analyses of spectral variations of peptide amide I vibrations (mainly amide C=O stretch) from which values for such coupling can be derived, assuming the diagonal force field (FF) is understood

* Corresponding author. Tel.: +1 312 996 3156; fax: +1 312 996 0431.
E-mail address: tak@uic.edu (T.A. Keiderling).

and the specific modes observed can be assigned [11,27–30]. The latter is facilitated by isotopic substitution (for example by means of ^{13}C on the amide $\text{C}=\text{O}$) which decouples the labeled residues from the bulk of the peptide modes [20,21,27,31–34].

Peptides and proteins have two predominant types of extended regular secondary structure, α -helices and β -strands. The β -strands are not autonomously stable, but form β -sheets that involve multiple strands, stabilized by cross-strand hydrogen bonding. Prediction of the cross-strand amide vibrational coupling in β -sheet structures, which combined with the intra-strand sequential coupling yields the characteristic, strongly split β -sheet amide I absorption bands, has been particularly difficult. In β -sheets the orientation of the polar amide groups is such that dipole coupling may well dominate, but at the same time, the cross-strand H-bonds provide a mechanical link that may impact both the diagonal and off-diagonal force constants. Although the α -helices apparently yield more uniform band-shapes, with less detectable splitting, even for these structures the relative contributions of hydrogen bonding and TDC to vibrational coupling remain a topic of study [30,35,36].

In general, spectral splittings due to off-diagonal couplings in real molecules will be convolved with non-degeneracies in the diagonal FF for groups that are not structurally identical. Such non-degeneracy can be approached in various ways, explicitly by DFT computation of modes for realistic coupled peptides, or implicitly by parameterization [27]. Simple dipole modeling could never represent such non-degenerate effects, but TDC can be added, ad hoc, to more realistic local FF modeling if desired. However, in such a complex case, sorting out the contributions of the diagonal and off-diagonal empirical FF approximations is necessary, if one wants to interpret experimental data in terms of coupling. This can be accomplished by careful comparison of TDC and quantum mechanically derived vibrational couplings for idealized structures whose end effects (non-uniformities) are treated consistently.

Such a systematic theoretical test will allow us to evaluate the degree of approximation being made when using the computationally simpler models based on TDC or, conversely, to establish the need to consider inter-amide couplings derived from more expensive, yet more accurate density functional theory, (DFT)-level quantum mechanical FFs. Computational methods of determining peptide FFs have developed so that highly reliable representations of IR spectra can be obtained for small to medium-sized peptides using DFT methods. We have extended these to longer peptides with regular structures by means of a property transfer algorithm [37,38]. Transferred DFT FFs have yielded quite accurate representations of helical spectra, and by use of isotope substitution (^{13}C on the amide $\text{C}=\text{O}$) have provided site-specific evaluations of amide I mode coupling that fits experimental IR and VCD data exceptionally well [18,20,21,32]. With model isotope-substituted systems, specific sites having virtually degenerate diagonal FF contributions can be singled out and decoupled from the rest of the peptide chain. This permits quite focused evaluation of coupling interactions [20]. For β -sheets we have had similar success, when the computations were compared to systems with extended flat sheet structures [39,40]. When sheets twist, the

spectra are highly variable and need more specific modeling. However, for the test cases we have studied, the amide I vibrational coupling between the β -strands, as evidenced in splitting of modes from isotopically labeled sites, is represented fairly well by use of uniform model structures [21].

In this paper we investigate the contribution of TDC to the inter-amide vibrational coupling derived from the DFT-level quantum chemical simulations of the vibrational spectra for model peptides forming helices and sheets. We directly compare the spectra obtained by full DFT computations with various approximations to them using DFT-level FF for small fragments combined with TDC coupling to simulate the longer range off-diagonal FF contributions. Putting DFT and TDC approaches on the same foundation with local (intra-residue and in some tests near-neighbor) coupling being represented for the same structures with two theoretical bases, provides a means of realistically evaluating the TDC approximation. It might be noted that Torii and Tasumi have previously reported that TDC only works for next near-neighbor couplings [41]. This further underlines the importance of putting the TDC approximation to a systematic test. In this study we evaluate the contributions of TDC by use of relatively high level (DFT) FFs and dipole moments for test molecules (see below) that approach experimentally interesting sizes. We do sequential calculations that gradually introduce TDC corrections to the FF transferred from DFT calculations on smaller fragments. The tests herein do not make any assumptions as to the size or orientation of the dipole, taking these values from the DFT results, rather than the scaling or parameterization to fit the theoretical [41] or experimental spectra [11,27,29,42].

2. Methods

2.1. α -Helical models

N-Methyl-acetamide (NMA) has often been used to model just the amide functional group. As a minimalist approach to simulation of a local peptide FF that does not contain any inter-amide vibrational couplings, we have transferred the NMA vibrational force constants, calculated at the DFT level. (It should be clear that our use of NMA transfer in this test does not endorse such an approach for explaining real spectra, but rather it provides a computational mechanism to allow testing of the TDC approximation. As will be shown this is an inadequate approach, but is one suggested by total reliance on TDC for inter-residue coupling.) Augmenting the NMA-based peptide FF with TDC corrections represents the simplest test of the TDC contribution to the amide vibrational interactions [43,44]. By using increasingly larger peptide models (di-, tri-amide, etc.) for calculations of DFT vibrational FF's the complete nearest and next nearest neighbor inter-amide couplings can be sequentially added into the models for testing. The peptides used in this comparative study are based on *L*-alanine (*L*-Ala), the smallest amino acid that contains a chiral α -carbon. The simplest of these is a di-amide, an *N*- and *C*-terminally blocked Ala molecule, Ac-L-Ala-NH-Me

(Me = CH₃), which offers the opportunity to model coupling and has been used for basic peptide models in the past [45].

The next step up in the oligopeptide complexity is a triamide (**A3**), Ac-(L-Ala)₂-NH-Me [38,46]. In these models the middle amide group interacts with its nearest neighbor amide groups on both N- and C-terminal sides. Since the central and two different terminal groups can be defined, the tri-amide represents a minimal model for a small fragment from which the DFT parameters can be used for simulations of sequential interactions which might be seen in spectra of larger molecules. Idealized α -helical **A3** models were constructed using standard values of the backbone ϕ , ψ , ω dihedral angles [46].

The tri-amide models (**A3**) do provide reasonable models of i , $i + 1$ and i , $i - 1$ nearest neighbor coupling and include some representations of 1–3 coupling but are too short to incorporate the intramolecular hydrogen bonding characteristic of α -helices. (Torii and Tasumi used a similar structure based on Gly as its largest model [41].) The shortest oligopeptides where both the carboxyl and amino groups of one amide linkage can form α -helical-like i , $i + 4$ hydrogen bonds is the hepta-amide (**A7**), Ac-(L-Ala)₆-NH-Me, which accordingly has been the basis for many of our previous α -helical spectral simulations [18,32,38,47]. The amino group of the central amide linkage of **A7** hydrogen bonds to the carboxyl of the terminal acetyl capping group while the carboxyl group of the central amide forms a hydrogen bond with the amino group of the C-terminal methylamide. In addition, three N-terminal residues are singly hydrogen-bonded through their carboxyl group and three C-terminal residues through the amino group. The standard conformational parameters were again used in these “minimal hydrogen-bonded” model helical structures.

Ideally we would like to compare TDC computations with full DFT calculations on long peptides, but of course this has practical limits. We have constructed and calculated spectra for helices as large as 50 residues and sheets as large as ~ 70 residues, but in these large molecule cases, we of course transferred DFT results from smaller peptides [37]. For the present report, the goal was direct comparison of TDC corrected to full DFT computed spectra, so the target chosen for the α -helical representation was an 11-amide helix, constructed as Ac-(L-Ala)₁₀-NH-Me (**A11**), for which we were able to obtain both full DFT computation of the FF and intensity parameters [20,48] as well as simulate spectra by transfer of parameters from the small molecules described above. We have numerous similar comparisons based on transfer from **A7** to a similarly conformed 21- (**A21** [18]) and 25-amide peptide [20] as well as other helical conformations (3_{10} - and 3_1 -helix), which will not be reported here for conciseness, but are available separately [32,49].

2.2. β -Sheet models

Anti-parallel β -sheet models used in DFT calculations were constructed from Ac-(L-Ala)₂-NH-Me (tri-amides) aligned in a three-stranded anti-parallel sheet structure (termed 3×3

model), whose conformation was derived from the crystal structure of β -sheet poly-L-alanine [50]. These structures are characterized by backbone torsional angles of $\phi = -138.56^\circ$, $\psi = 134.55^\circ$ and $\omega = -178.53^\circ$, and interstrand hydrogen bond distances (O...H) of 1.898 Å [39,49]. While transfer to larger structures can be done [31,39,40] we will focus here on the 3×3 model, since DFT computations were possible for this size molecule at that time. Reference to published results can serve for comparison to the results for large multi-stranded β -sheets [39]. Since the 3×3 model is impacted by end effects, it might not provide a good test of long-range coupling. Thus we have also computed comparative spectra for a longer, two-stranded sheet of six amides each, that we term the 2×6 model. This was the largest full DFT calculation we have done, possible by use of C₂ symmetry, with a structure obtained initially with the same ϕ , ψ angles but then DFT optimized [31].

2.3. Density functional theory (DFT) calculations

All quantum mechanical calculations were carried out at the DFT level, using the Gaussian 98 or Gaussian 03 program package [51]. The BPW91 density functional [52–55] with 6-31G* basis set was used in all cases. This somewhat simpler (non-hybrid) functional optimizes computation of the amide I and II modes, both in accuracy and speed of computation, but may not be optimal for lower frequency modes, should they be of eventual interest. Clearly for the case at hand, with its focus on amide I coupling, an approach such as this which yields a more accurate diagonal FF is preferable. Most likely use of a diffuse basis set (e.g., 6-31++G**) in a future test would improve representation of the H-bonding and of the diagonal FF and frequencies [31,56].

Prior to the vibrational FF and intensity calculations, NMA was fully optimized at the BPW91/6-31G* level. The geometries of **A3** and **A11** were fully optimized except that the (ϕ , ψ , ω) angles were constrained to the standard (idealized) -57° , -47° , 180° α -helical values. Similarly the β -sheet model was constrained to the initial poly-Ala (ϕ , ψ , ω) values (see above) for each strand. For the 3×3 model the inter-strand hydrogen bonds were likewise constrained to the initial value [39], while that of the 2×6 model was optimized [31]. These constrained geometries were optimized to the default optimization convergence criteria of Gaussian 98; and for the resulting structures the analytical, harmonic FF and analytical APT were calculated at the same level of theory. AAT parameters, which are needed for VCD simulation, were also calculated as implemented in Gaussian 98 following the methods of Stephens [57–59]. Since VCD will not be the focus of this paper, no additional discussion of it will be made here, but simulated VCD spectra can be obtained from our results, as discussed previously [20,39,49]. Early calculations were carried out on a previous University HP 9000/800 computer and later ones on one of several PC-Linux clusters typically using 4–6 CPUs per calculation. For example, the FF calculation of the 3×3 peptide (96 atoms, 45 heavy atoms, 930 basis functions) took 10–15 days of wall-clock time (CPU time 8.5 days) using

4-CPU's of the HP 9000/800 and the energy optimization and FF for the 2×6 model, same basis set, took ~ 2 weeks on a single Linux processor (3 GHz, 4 GB).

2.4. Transfer of spectral parameters

The spectral frequencies and intensities of **A11** were available directly from DFT computation, and for testing the TDC model were also simulated using transfer of the DFT calculated FF, APT and AAT matrices from **A3** and from NMA by means of our now standard property tensor transfer methods [37]. Similarly the FF, APT and AAT of 3-strands of three amides each (3×3) β -sheet model and the two-stranded (2×6) β -sheet were calculated directly with DFT and by transfer of parameters from NMA and from corresponding single β -strand. These transfers test the neglect of the off-diagonal terms in the FF both intra- and inter-strand (transfer from NMA) and inter-strand (or cross-strand) only (transfer from a single β -strand) and correcting for them with the TDC model. Larger calculations, for example, considering 21-amide helices constrained to α -, 3_{10} - and 3_1 -helical (poly-L-Pro II like) geometries with transfers from both **A3** and **A7** were also carried out and are reported in a thesis [49]. Larger fully optimized DFT calculations of several 10-amide helical peptides are also available, but the geometries differ due to the minimization [48].

2.5. Transition dipole coupling (TDC) correction

The transferred FF incorporates only the interactions between atoms encompassed in the small fragment that is the source of the transferred parameters. In other words, the FF is a matrix with inter-amide coupling elements only on or near to the diagonal. Thus for transfer from NMA there are no elements between amides, only cross-terms between atoms within an amide. This provides a convenient form for testing the contribution of transition dipole coupling (TDC) by filling in the long-range off-diagonal zeros resulting from the transfer with values obtained via the TDC. Comparison of these results to those obtained with full DFT calculation provides the evaluation basis.

The approach used here for correcting the transferred FF by TDC is different from the empirical TDC-based coupled oscillator models in that it is non-perturbative and uses no empirically adjusted parameters. Note that TDC terms approximate only the interaction constants that are unknown, since they correspond to the atomic pairs beyond the span of the smaller molecule from which the FF is transferred, and thus have been set to zero. If the transfer is from NMA, TDC would be used to determine all off-diagonal amide couplings, but if from **A3**, for example, it would only be used for long-range values. The TDC terms are substituted for just the zero elements (C=O couplings only for this test) of the transferred Cartesian FF matrix. The full FF matrix, including local DFT (transferred) and long-range TDC components, is then diagonalized. The dipole derivatives are the DFT-level APT values, which fixes their magnitude as well as orientation. The

only remaining problem is the position of the transition dipole moments. Since the APT is an atomic property, a natural choice is to assign the position of the transition dipole to each atom, which we use here, but have also compared them to other choices, as we have discussed elsewhere [49]. Then, the TDC corrected FF can be written in terms of the Cartesian APT as:

$$f_{A\lambda, B\xi}^{\text{TDC}} = \frac{\partial U^{\text{TDC}}}{\partial X_{A,\lambda} \partial X_{B,\xi}} \approx \frac{1}{\epsilon R_{AB}^3} \left[\sum_{i=x,y,z} \frac{\partial \mu_i^A}{\partial X_{A,\lambda}} \frac{\partial \mu_i^B}{\partial X_{B,\xi}} - 3 \times \sum_{i,j=x,y,z} \left(\frac{\partial \mu_i^A}{\partial X_{A,\lambda}} e_{AB,i} \right) \left(\frac{\partial \mu_j^B}{\partial X_{B,\xi}} e_{AB,j} \right) \right]$$

for all pairs of atoms A, B whose force constants are absent in the transferred FF. Here $X_{A,\lambda}$, $\lambda = [x, y, z]$ are Cartesian displacements of the atom A , and $\partial \mu_i / \partial X_\lambda$ are the components of the APT. The relative dielectric constant ϵ was chosen as 1 to maximize coupling and to reflect the conditions of the DFT calculation to which this is compared.

2.6. Simulation of the IR absorption

Spectra were computed by transfer of FF parameters onto molecular coordinates, diagonalization of the FF and convolution of the resulting normal modes with APT and AAT values. These manipulations were performed using a set of programs, running under UNIX (by Petr Bour). The final IR and VCD band profiles are obtained in all cases by summing over normal modes each represented by lineshapes having a constant width but areas proportional to the dipole strengths, D .

3. Results

3.1. Helical peptides

In Fig. 1 are compared the IR of the amide I transitions for **A11** obtained with DFT (a), transfer from **A3** (b) and the same with augmentation by the TDC correction (c). The important overall observation is that the dispersion of the modes changes significantly between the full DFT model and the truncated FF, even when corrected with TDC. In the full DFT computation, as seen experimentally, most of the amide I intensity is in a mode that is polarized along the helix axis and whose frequency lies in the center of the exciton dispersed amide I profile. When the **A3** FF is used, resulting from the diagonal FF terms the **A11** amide I frequencies are higher, presumably due to the lack of H-bonds in the **A3** model, but secondarily due to the relatively weak helical macro dipole. But if one neglects the overall amide I frequency shift and focuses on the comparison of bandshapes which result from coupling, the dispersion is much less and the intense mode is displaced to the high frequency edge of the dispersed modes for the **A3** transferred case. Many more modes have significant dipole strength, due to the less extensive exciton coupling resulting from shorter-range coupling. This is evident in the nature of the modes which tend to be localized on

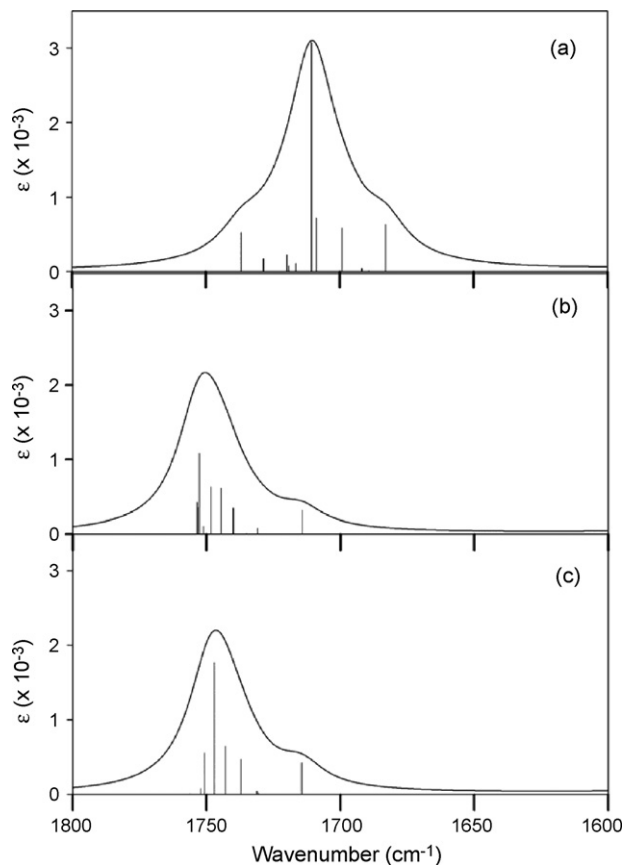


Fig. 1. Comparison of amide I IR spectra for **A11** obtained with a full DFT calculation (a), with transfer from **A3** (b), and with transfer from **A3** plus addition of TDC corrections (c).

3–4 amides with the **A3** transfer. Adding TDC to the **A3** FF adds longer range coupling and does shift more of the intensity into one (or a few) dominant transitions, in better agreement with the DFT result, but the most intense component is still one of the higher frequency modes. It is important to realize that the results shown here for TDC, which keep the near-neighbor coupling at the DFT level by use of **A3** as a model, should be roughly equivalent to the Torii and Tasumi correction [41]. With DFT-determined dipole moments, TDC remains inadequate to reproduce the dispersion, which depends on the long-range coupling. The lowest frequency mode with significant intensity is in all cases the N-terminal amide, due to an end effect (diagonal) not to coupling.

By use of a transfer from **A3**, DFT-level local coupling is always maintained. We next transferred spectral parameters from NMA onto the **A11** structure to create a peptide for which there is no sequential (through-bond) amide coupling. Then, to add coupling, we added TDC (through-space) off-diagonal terms as described. Comparison of the results to the fully DFT computed **A11** spectra is shown in Fig. 2. Qualitatively the same problem exists, but to a larger extent. With transfer from NMA, we get the “group frequency” for the amide I, but there is no inter-amide coupling from the FF, which results in very little dispersion ($\sim 10 \text{ cm}^{-1}$). With addition of TDC the dispersion modestly increases (to $\sim 20 \text{ cm}^{-1}$), but in both cases remains very much less than the $\sim 60 \text{ cm}^{-1}$ seen with the

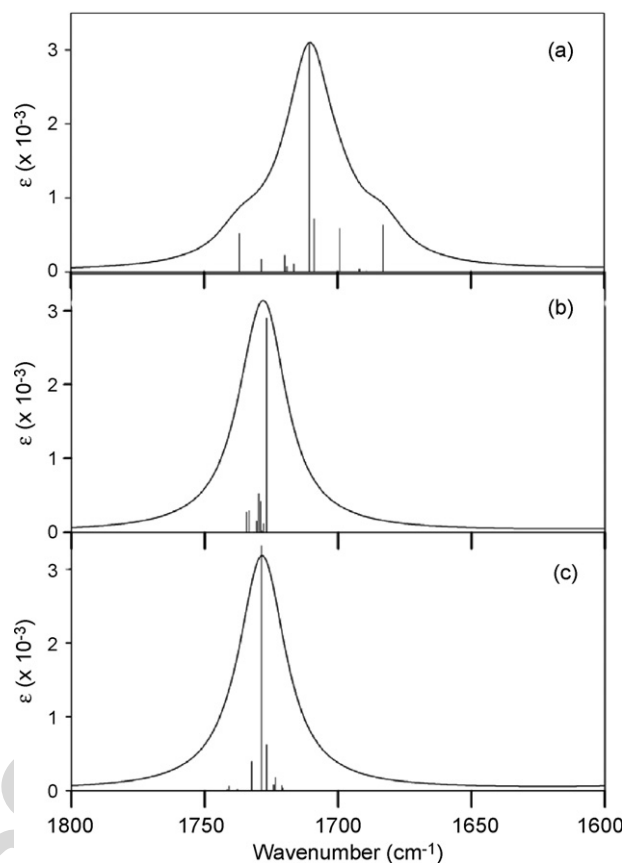


Fig. 2. Comparison of amide I IR for **A11** obtained from a full DFT calculation (a), by transfer from NMA (b), and by transfer from NMA augmented with TDC corrections (c).

DFT parameters. This dispersion has always been a characteristic of our fully DFT and transfer-computed peptide amide I spectra, as we have previously noted [38,39,47], but has been also noted in empirical studies [36,60]. Clearly this is a flaw in traditional “group frequency” approaches to interpretation of protein and peptide IR spectra where single frequencies are assigned to given species or conformations, and the dispersion of the band cannot be taken into account.

Another way to look at the effect of TDC versus DFT coupling is to compute the interaction of two amides directly without any mechanical coupling. We have done this by placing two NMA molecules on successively separated amides in a helix and computing the FF and APT parameters at the DFT level. While this does not correspond to an isolatable molecule, these pairs of amides couple via the electronic structure computation and represent a separation of electronic through-space and -bond effects. We can model this interaction classically by just placing the same NMA molecule on both positions and computing the interaction between the positions with TDC, using the APT-derived dipoles as a basis. The results of such a computation are summarized in Table 1. Full DFT calculation of the interaction between $i, i + 1$ positions cannot be done since the NMA molecules would overlap, but it can be simulated by computing the splitting for the two amide I modes in Ac-Gly-NH-Me (**G2**), which most closely resembles the two “touching” NMA molecules. However, this approximation

Table 1
Amide I for two NMA positioned on a helix at various sequential separations

Label positions	Isolated 2 NMA			TDC correction			DFT		
	$\nu_{\text{high}}, \nu_{\text{low}}$	$\Delta\nu$	$D_{\text{high}}, D_{\text{low}}$	$\nu_{\text{high}}, \nu_{\text{low}}$	$\Delta\nu$	$D_{\text{high}}, D_{\text{low}}$	$\nu_{\text{high}}, \nu_{\text{low}}$	$\Delta\nu$	$D_{\text{high}}, D_{\text{low}}$
$(i, i + 1)^{\text{a}}$	1735.2	2.6	0.022	1737.1	6.2	0.078	1755.5	17.4	0.059
	1732.6		0.078	1731.0	(5.6) ^b	0.022	1738.1		0.024
$(i, i + 2)$	1737.9	3.1	0.049	1738.2	3.5	0.037	1725.4	16.7	0.038
	1734.8		0.049	1734.7	(1,7) ^b	0.062	1708.7		0.078
$(i, i + 3)$	1737.9	0.03	0.049	1742.2	8.5	0.007	1723.1	10.5	0.001
	1737.8		0.048	1733.8		0.090	1712.6		0.144
$(i, i + 4)$	1737.9	0.08	0.080	1738.7	1.6	0.004	1726.8	1.8	0.012
	1737.9		0.017	1737.1		0.094	1724.9		0.103
$(i, i + 5)$	1738.0	0.12	0.027	1738.4	1.0	0.025	1730.9	1.3	0.028
	1737.8		0.071	1737.4		0.073	1729.6		0.077

Comparisons of DFT and TDC coupling. ν_{high} and ν_{low} are two frequencies in cm^{-1} and $\Delta\nu$ is the frequency difference between them. D_{high} and D_{low} are corresponding dipole strength in Debye².

^a Frequencies are determined with Ac-Gly-NH-Me (G2).

^b Calculated $2V$ where V is the coupling constant.

does introduce mechanical and other electronic coupling that is not in any non-bonded approach. With TDC such near-neighbor coupling poses no particular computational problem, but obviously misses out on what must be the most significant inter-amide interaction due to mechanical (bonding) effects. This accounts for the drop in interaction from $\Delta\nu \sim 17 \text{ cm}^{-1}$ (G2) to $\sim 6.2 \text{ cm}^{-1}$ for two NMA dipoles interacting via TDC (Table 1). For $i, i + 2$ interactions, the NMA₂ DFT splitting is $\Delta\nu \sim 17 \text{ cm}^{-1}$, while that from TDC is only $\sim 4 \text{ cm}^{-1}$, implying a surprising level of electronic interaction between non-bonded groups. It is clear that the assumption that TDC can adequately represent next-nearest neighbor coupling is dependent on a model, presumably inclusion of some through-bond coupling via the transfer from a three amides model would reduce the dramatic shortfall in coupling seen here [41]. This reminds one of the consequences previously noted in a study of VCD of coupled oscillators where the simple dipole model broke down for close lying dipoles [61]. In the present case based on transfer from NMA, however, the distances are larger and the mechanical coupling is gone. However, for $(i, i + 3)$; $(i, i + 4)$ and $(i, i + 5)$

the TDC determined splitting, 8.5, 1.6, 1.0 cm^{-1} , is virtually the same as that from the DFT computation, ($\Delta\nu$ 10.5, 1.8, 1.3 cm^{-1} , respectively, suggesting that such long-range coupling may indeed be mostly dipolar in nature, even when represented by DFT-derived dipole moments. The very small size of these couplings does suggest that the comparison should be made with caution.

These sorts of patterns were explored previously in our discussion of isotope labels in helical 25-amide peptides [20], where the coupling of different positions was determined both with DFT-based FF and by TDC (there using a simpler method, but obtaining similar results). We have looked at this labeled C=O coupling issue again, but now with the models computed above, i.e. **A11** all DFT and **A11** transfer from NMA and **A3** DFT. This comparison is summarized in Table 2 for substitution of a single ¹³C=O labeled group (**1L**, substituted on position 6) and of two such groups either sequentially (**2LT**, positions 6, 7 or $i, i + 1$), alternate (**2L1S**, positions 5, 7, $i, i + 2$) or separated by two ¹²C=O groups (**2L2S**, positions 5, 8, $i, i + 3$). In the previous study as well as this one, the coupling falls off with

Table 2
Coupling of isotopically labeled amide I modes in a helix

Position	DFT			Transferred from A3			Transferred from A3 + TDC corrected			Transferred from NMA		Transferred from NMA + TDC corrected		
	$\nu_{\text{high}}, \nu_{\text{low}}$	$\Delta\nu$	$D_{\text{high}}, D_{\text{low}}$	$\nu_{\text{high}}, \nu_{\text{low}}$	$\Delta\nu$	$D_{\text{high}}, D_{\text{low}}$	$\nu_{\text{high}}, \nu_{\text{low}}$	$\Delta\nu$	$D_{\text{high}}, D_{\text{low}}$	$\nu_{\text{high}}, \nu_{\text{low}}$	$D_{\text{high}}, D_{\text{low}}$	$\nu_{\text{high}}, \nu_{\text{low}}$	$\Delta\nu$	$D_{\text{high}}, D_{\text{low}}$
1L (6) ^a	1656.7		0.049	1697.4		0.026	1697.5		0.033	1685.1	0.052	1684.3		0.051
2LT (6, 7)	1666.2	15.3	0.132	1705.7	14.2	0.058	1705.1	13.2	0.079	1686.2	0.014	1688.5	7.7	0.106
	1650.9		0.010	1691.5		0.010	1691.9		0.011	1684.0	0.087	1680.8		0.014
2L1S (5, 7)	1659.8	5.0	0.025	1700.6	5.80	0.025	1700.0	4.6	0.028	1685.1	0.026	1684.9	1.1	0.029
	1654.8		0.071	1694.8		0.029	1695.4		0.038	1685.0	0.079	1683.8		0.073
2L2S (5, 8)	1659.9	4.8	0.013	1698.2	1.4	0.050	1699.0	2.8	0.007	1685.1	0.009	1687.8	6.5	0.009
	1655.1		0.088	1696.8		0.006	1696.2		0.057	1685.0	0.096	1681.3		0.084

Symbols as in Table 1.

^a The numbers in parenthesis represents the position of ¹³C in **A11** helix.

increased separation along the chain. This is of course expected, but given the helical structure, the $i, i + 4$ structure might have been assumed to have a shortening of the distance compared to the $i, i + 3$. In fact this does not happen, and both the DFT and TDC values progressively decrease [20]. Similarly, all these coupling constants have a negative sign, except for $i, i + 1$. The **A3** transfer gives almost the same coupling for the neighbor and next near-neighbor (**2LT** and **2LIS**) cases as does the full DFT, but the longer range **2L2S** case is modeled too low with the transfer and even with TDC added. Again TDC based on DFT computed dipole moments are insufficient to make up for the missing coupling, even for residues $i, i + 2$ in the sequence, in sharp contrast to earlier conclusions [41]. Transfer from NMA plus TDC is much worse for the short-range couplings, but unexpectedly is better for the longer range one.

3.2. β -Sheet models

A series of test calculations was performed on the 3×3 β -sheet using a transferred DFT-level FF from NMA for each amide group and the TDC correction based on the DFT values of transition dipole strengths (APT) [39,49] as coupling terms. Alternatively, the DFT FF from a single strand calculation was transferred onto the three-stranded model and the TDC used only for inter-strand coupling. The amide I IR results comparing these models are shown in Fig. 3. The transfer from NMA alone or even with TDC yields narrow intensity distributions (Fig. 3a and b), albeit with a major intensity component being the lowest frequency mode, which is in agreement with the DFT and with experimental expectations. The TDC, here within and between strands, adds about 15 cm^{-1} of splitting to the NMA derived modes. If one instead takes a

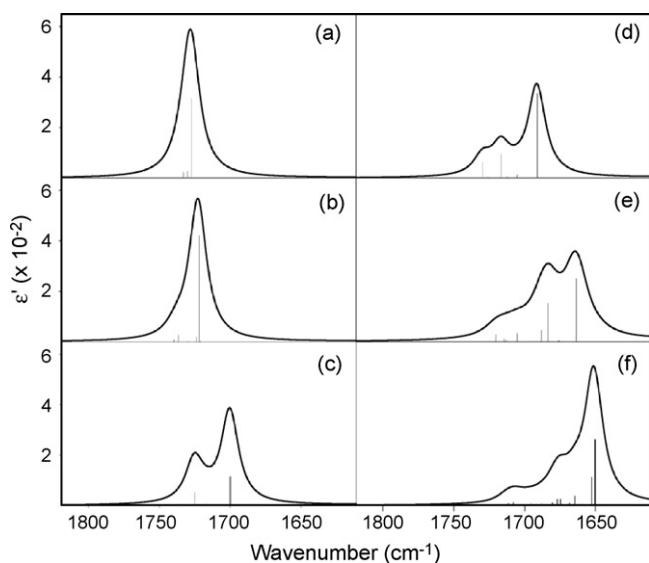


Fig. 3. Comparison of Amide I IR for the 3×3 β -sheet model calculated using transfer of parameters from NMA (a), transfer from NMA plus TDC calculated using NMA transition dipole moments (APT) (b), transfer from DFT calculations on 1×3 single strand of three amides (c), transfer from 1×3 plus addition of TDC cross-strand corrections (d), full DFT calculation of 3×3 (e), and transfer from full DFT calculation of 3×3 to 5×8 sheets (f).

single strand calculation and transfers it to each of the three strands, so that the intra-strand coupling is represented at the DFT level, then a significant intensity distribution (splitting) results (Fig. 3c). If one then adds TDC to represent the cross-strand coupling, a band profile is achieved (Fig. 3d) that suggests the large dispersion expected for a β -sheet, as represented in the full DFT calculation (Fig. 3e). However, the details of the modes do differ between them and the TDC-induced dispersion is less than 40 cm^{-1} (Fig. 3d), adding only about 10 cm^{-1} to the 1×3 dispersion (Fig. 3c), while that with the DFT computation is $\sim 60 \text{ cm}^{-1}$ (Fig. 3e), reflecting the basic character of an anti-parallel β -sheet structure. As shown earlier [39], if more strands are added to the model, the dispersion increases and the intensity of the characteristic low frequency mode grows. These are necessarily modeled by transfer, here shown from the 3×3 -DFT calculations to the 5×8 sheets (Fig. 3f) for comparison.

To parallel the above helical computations, we also transferred NMA and Ac-Ala₂-NH-Me (1×3) parameters to the 2×6 sheets structure and then added TDC corrections to see how these compared to the full DFT computation for 2×6 , an extended two-strand hydrogen-bonded β -structure. This has particular interest in terms of modeling isotopic substitutions, as we have studied recently [21,31]. Here the pattern is dramatically different, as the NMA transfer alone and with TDC yields a

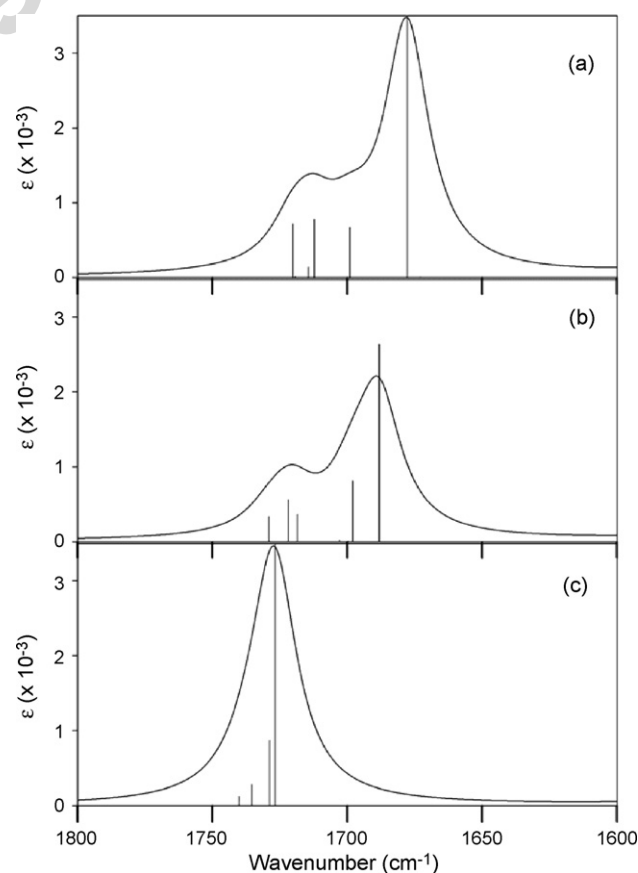


Fig. 4. Comparison of Amide I IR for 2×6 β -sheet model obtained by a full DFT calculation (a), by transfer from 1×3 β -strand plus TDC corrections (b), and by transfer from NMA plus TDC corrections (c).

dispersion of only ~ 10 and ~ 20 cm^{-1} , respectively, (Fig. 4c) while the full DFT result is nearly 50 cm^{-1} (Fig. 4a), approaching what we have observed in hairpin peptides (~ 50 cm^{-1}) [21,62]. However, transferring parameters derived from a DFT computation for a single strand (1×3) yields much more realistic dispersions, ~ 30 and 40 cm^{-1} , before and after addition of TDC, respectively (Fig. 4b). There are a great many possibilities for isotopic substitution in 2×6 , some of which form H-bonded rings of $^{13}\text{C}=\text{O}$ groups that are cross-strand coupled, as was the topic of our recent hairpin study [21] and others that yield couplings in less obvious ways [31]. In summary, the DFT computed couplings are almost always larger than for the TDC transferred models whether based on FF from NMA or 1×3 . Certainly without the 1×3 , the couplings between sequential positions in a strand are severely underestimated, much as seen for helices. The cross-strand and long-range in-strand couplings are also underestimated, but in that case they are often within a factor of two, and for $\text{C}=\text{O}$ groups on opposite strands forming a 10-member H-bonded ring, they are much closer. Given the complexity of defining all these positions and the dependence of the actual values on specific geometrical constraints, we have chosen to discuss them only globally at present.

4. Discussion

4.1. Helices

The relatively small changes caused by addition of the approximate force constants, to account for those missing when the FF from a modest-sized peptide fragment is transferred onto a larger molecule, are consistent with the vibrational FF being dominated by local interactions. The fact that these corrections approach each other at long range is consistent with the short-range effects having a different origin. (However, in the process of reaching agreement, they are essentially approaching zero, which could imply they are approaching the confidence limit of the calculations. In other words, this observation would be more convincing if the DFT and TDC were similar for large values of the coupling as well.) A significant aspect of the difference is the missing H-bonds in the **A3** and NMA transfers (even when TDC corrected) but which are represented quite fully in the DFT of **A11**. These have an impact on the diagonal FF, but also offer a unique path for mechanical coupling between distant residues. Further, in the 3_{10} helix and 3_1 helix calculations, (data not shown), these effects of TDC correction are actually less than for the α -helical data presented here [49]. The α -helix represents a compact conformation, as perhaps best evidenced by the small translation per residue for this structure resulting in the sequential amide groups being spatially closer than in other helical structures. Moreover, the polar amide groups are highly aligned in the α -helix, which results in a strong helical macrodipole that maximizes electrostatic interaction between these groups. The polarity of the α -helix may be also the reason why the lowest frequency amide I modes are consistently N-terminal amide modes. (It might be noted that the 3_1 -helical results (not shown) are the least affected by TDC addition or the length of the model peptide used to transfer onto a larger molecule. This could reflect

its lack of helical dipole, resulting from its $\text{C}=\text{O}$ groups pointing out into solution away from the helical axis.)

Our interest and ability to determine amide coupling arose from isotopic substitution experiments and the subsequent theoretical analyses [20,21,31,32]. In this comparison, it is clear that the full DFT of **A11** and the **A3** transfer yield similar isotopic coupling results for the near neighbors, while the NMA and TDC corrections fall short (factor of 2) in this regard. None the less, the patterns developed by substituting two NMA molecules on a helix indeed follow the long-range pattern of dominance by dipolar coupling interactions. One might assume that addition of a larger dipole should correct for this fall off. That might work, except that it would require a variable correction for sites close and those far apart.

Our choice for the placement of bond dipoles on atom sites, reflecting the APT definitions, in fact, bears some resemblance to the distributed origin gauge method, proposed by Stephens [63] for eliminating the uncertainty in the proper origin choice for gauge dependent AAT. Other possibilities for the choice of the transition dipole moment position are possible. For example, the APT element, calculated for the small fragment represents a contribution of the motion of a particular atom to the transition dipole of the whole small fragment molecule. Thus, a physically sound choice of the transition dipole moment position is in the center of the “best” fit between the large and small molecules, which is used for the transfer of the particular APT. To test the dependence of the resulting TDC corrected spectra for large oligopeptides on the particular selection of the transition dipole moment origin, both the above possibilities were implemented and compared (results not shown, [49]). In essence these origin corrections showed little difference from the TDC computations made in a manner paralleling the methods reported above. Such effects do not appear to be the major concern, but rather the model itself is one that should be interrogated.

An alternate approach to correcting for long-range effects is the use of semi-empirical (PM3 parametrization) interaction constants in those parts of the FF matrix where our transfer methods leave zero elements. While probably providing a better approximation than TDC for long-range terms, PM3 is certainly less accurate than DFT. However, given the apparent agreement of long-range TDC and DFT coupling constants, such errors may well be negligible when separations of more than a few residues are considered. (For example, PM3 calculated vibrational frequencies for a 21-amide helix, **A21**, are ~ 1890 and ~ 1480 cm^{-1} for the amide I and II, respectively, compared to ~ 1730 and ~ 1520 cm^{-1} for transfer of the **A7** FF.) A comparison of PM3 and TDC corrections shows a small shift of the diagonal FF (center frequency of the amide I band) but little observable effect on the dispersion for **A21** transferred from **A7** [49]. In other words, the main interactions are local and the long-range correction is minor.

4.2. Sheets

While it is tempting to ascribe the predicted trends seen in the amide I IR bandshapes of β -sheets to strong H-bonding

between β -strands, our results show that the origin is more complex. Because the split character of the IR amide I band is observed in the single-stranded simulations, it cannot be solely due to the hydrogen bonding. This would be consistent with findings of Moore and Krimm [42] who empirically added non-bonded, transition dipole coupling (TDC) interactions to the force field in order to explain this bandshape. However, as also pointed out [44,64], perturbative treatments based on TDC alone [36,42,65] are not sufficient to explain certain important details of amide I spectra.

The difference here may be the magnitude of the TDC between strands, thus the functionality may have the right form, but the magnitude is reduced. That is actually a reasonable issue since the NMA and single strand models may have reduced dipole strength due to the lack of H-bonds enhancing the C=O dipole. In the helical case above, all residues were alike, but in a sheet, the cross-strand interactions are very different from the intra-strand ones, as noted long ago [66]. Recent empirical modeling of protein vibrational spectra by Mendelsohn and coworkers have treated such interactions separately [28] and more recently distinguished between diagonally perturbed amide I modes on different positions [27].

Comparison to the spectra obtained from the full DFT calculation (Fig. 3c) shows that the calculated IR bandshapes cannot be explained by TDC. If the splitting were only due to the TDC, the high frequency amide I components would shift further up and the lower frequency ones further down, thus maintaining the center frequency of the band. On the other hand, in the DFT simulations both components shift to the lower frequencies (the high frequency one only slightly) as more strands are added. Furthermore, the component splitting is significantly underestimated, $\sim 15\text{ cm}^{-1}$, if only the TDC were included as the mode coupling mechanism (Fig. 3b), and $\sim 38\text{ cm}^{-1}$ for TDC coupling between strands (Fig. 3d). One of the reasons for this underestimated splitting is the smaller transition dipole moment computed for the NMA, as compared to the empirical values obtained from experiment and used in empirical TDC calculations. Chirgadze and Nevskaya [65] use the amide I transition dipole moment value of 0.39 Debye, calculated from the absorption intensity of β -polypeptides, while that calculated for the NMA (at BPW91/6-31G* level) is 0.22 D. It has been shown [49] that this theoretical value corresponds very well to the experimentally measured dipole strength of NMA in acetonitrile and thus probably also that in the gas phase. From the results presented above it is obvious that the amide I intensity, per amide group, increases with the size of the sheet: for example, the integrated transition dipole moment per amide group for the anti-parallel, 3×3 β -sheet from the ab initio calculation is 0.24 D, and for the 5×8 anti-parallel β -sheet 0.33 D. Obviously, the larger values of transition dipole moments in larger sheets (0.39 is expected for infinite sheet [49]) are a consequence of amide mode coupling, creating an overall dipole the modes couple to, and cannot arise from TDC which would conserve dipole moment among coupled modes. Thus, to correct the TDC, using a larger dipole moment is sensible, but the source of dipole must be from a coupled mode already determined, not one derived from

the isolated dipole one might conveniently compute. This leads to a logical fault, since once the larger system is computed, it could just as well be used for the vibrational modeling by means transfer of the DFT computed local interactions as we have done. Unsurprisingly, when only TDC is assumed with the transition dipole moment value of 0.39 D (infinite helix value) (Fig. 3b), nearly perfect correspondence with the results of Chirgadze and Nevskaya [65] for the 3×3 anti-parallel β -sheet is obtained. However, the resulting bandshape is significantly different than that obtained from the full DFT calculation (Fig. 3c), in particular, the frequency of the amide I band maximum is higher. In addition, if full intrastrand interactions are included, the amide I band splitting becomes even larger ($\sim 70\text{ cm}^{-1}$) with this transition moment value (analogous to Fig. 3e). Using an empirical value of the transition dipole strength thus can improve amide I IR bandshape prediction, especially if the intra-strand coupling is modeled at the DFT level.

From these test calculations, for which we have employed non-empirical, DFT calculated parameters, it follows that both bonded and non-bonded interactions are necessary for prediction of proper IR bandshapes. This result is consistent with Miyazawa's original model [66] and with empirical parameterized calculations by Mendelsohn and coworkers that required both through-bond (including H-bonds) and TDC interactions to reproduce the amide I bandshapes of ^{13}C isotopically labeled β -sheet oligopeptides [28]. In a more recent study they have used an expansion of this method to obtain an excellent agreement with several experimental amide I contours for proteins using combined through-bond and electrostatic coupled oscillator model [27]. Where in this progression of studies is our work then? We are getting these various couplings not from some sort of empirical fit, but from DFT computations on realistically conformed peptides that provide the basis of the entire FF. This provides a more systematic test of the contributions by comparing the TDC corrected FF to the full DFT result on the same molecule with same electronic structure.

5. Conclusion

In conclusion, our calculations demonstrate that transition dipole coupling alone cannot explain the mode couplings that give rise to the amide I bandshapes characteristic for the α -helical and β -sheet peptide structures. It seems clear to us that to reproduce the spectral bandshapes, additional interactions, namely the through-bond effects, including both covalent and hydrogen bonds, play an important role. The question for the future is whether these effects can be reliably represented by empirical coupling schemes with a few parameters, or whether more complete electronic structure calculations are necessary. In particular, as one addresses the problem of irregular structures, a critical issue arises as to how important are the conformational variation in the diagonal FF [67]. These considerations could impede attempts to model proteins and poorly folded structures [27,30]. Added complications may include the effects of solvent and side-chains. For example, a

partially solvent exposed helix or sheet in a protein may exhibit quite different (diagonal) FF between the buried and exposed parts, and solvent may screen the electrostatic as well as weaken the H-bonding. While quantum chemical methods do not offer a straightforward way to separate individual “physical” contributions to the oscillator coupling (‘physical’ here means from the point of view of classical oscillator with classical coupling interactions), as demonstrated here, test calculations can be designed to investigate various effects, such as long-range electrostatic contribution. On the contrary, the strength of our parameter free, non-empirical approach is that the multitude of such contributions to the vibrational properties is not “adjusted” into a few empirical parameters. For example, by tuning the strength of TDC as shown for the β -sheet models, the agreement with the full quantum mechanical calculations can be improved, but such improvement may be misleading and one may miss important effects. Finally, one must eventually account for solvent effects, which in the case of water have a significant effect on the amide dipole moments and a difficult to model dielectric interaction, both of which presumably impact on coupling.

Acknowledgements

This work was supported in part by a grant to TAK from the National Science Foundation (CHE03-16014) and was assisted by a Fellowship to TAK from the John Simon Guggenheim Foundation. We wish to thank Ms. Rong Huang for help with some of the TDC calculations and with the manuscript preparation.

References

- [1] A. Barth, C. Zscherp, *Quart. Rev. Biophys.* 35 (2002) 369–430.
- [2] P.I. Haris, in: B. Ram Singh (Ed.), *Infrared Analysis of Peptides and Proteins: Principles and Applications*. ACS Symposium Series, ACS, Washington, DC, 2000, pp. 54–95.
- [3] F. Eker, X. Cao, L. Nafie, R. Schweitzer-Stenner, *J. Am. Chem. Soc.* 124 (2002) 14330–14341.
- [4] R. Schweitzer-Stenner, F. Eker, Q. Huang, K. Griebenow, *J. Am. Chem. Soc.* 123 (2001) 9628–9633.
- [5] S.A. Asher, A. Ianoul, G. Mix, M.N. Boyden, A. Karnoup, M. Diem, R. Schweitzer-Stenner, *J. Am. Chem. Soc.* 123 (2001) 11775–11781.
- [6] X.J. Zhao, T.G. Spiro, *J. Raman Spectrosc.* 29 (1998) 49–55.
- [7] R.W. Williams, *Meth. Enzymol.* 130 (1986) 311–331.
- [8] S. Woutersen, P. Hamm, *J. Phys. Chem. B* 104 (2000) 11316–11320.
- [9] S. Woutersen, P. Hamm, *J. Chem. Phys.* 114 (2001) 2727–2737.
- [10] S. Woutersen, P. Hamm, *J. Phys.: Condens. Matter* 14 (2002) R1035–R1062.
- [11] C. Fang, J. Wang, A.K. Charnley, W. Barber-Armstrong, A.B. Smith III, S.M. Decatur, R.M. Hochstrasser, *Chem. Phys. Lett.* 382 (2003) 586–592.
- [12] D.S. Talaga, W.L. Lau, H. Roder, J.Y. Tang, Y.W. Jia, W.F. DeGrado, R.M. Hochstrasser, *Proc. Natl. Acad. Sci. U.S.A.* 97 (2000) 13021–13026.
- [13] C.M. Cheatum, A. Tokmakoff, J. Knoester, *J. Chem. Phys.* 120 (2004) 8201–8215.
- [14] W. Barber-Armstrong, T. Donaldson, H. Wijesooriya, R.A.G.D. Silva, S.M. Decatur, *J. Am. Chem. Soc.* 126 (2004) 2339–2345.
- [15] S.M. Decatur, *Biopolymers* 54 (2000) 180–185.
- [16] S.M. Decatur, *J. Antonic*, *J. Am. Chem. Soc.* 121 (1999) 11914–11915.
- [17] R.A.G.D. Silva, W. Barber-Armstrong, S.M. Decatur, *J. Am. Chem. Soc.* 125 (2003) 13674–13675.
- [18] R.A.G.D. Silva, J. Kubelka, S.M. Decatur, P. Bour, T.A. Keiderling, *Proc. Natl. Acad. Sci. U.S.A.* 97 (2000) 8318–8323.
- [19] C.Y. Huang, Z. Getahun, T. Wang, W.F. DeGrado, F. Gai, *J. Am. Chem. Soc.* 123 (2001) 12111–12112.
- [20] R. Huang, J. Kubelka, W. Barber-Armstrong, R.A.G.D. Silva, S.M. Decatur, T.A. Keiderling, *J. Am. Chem. Soc.* 126 (2004) 2346–2354.
- [21] V. Setnicka, R. Huang, C.L. Thomas, M.A. Etienne, J. Kubelka, R.P. Hammer, T.A. Keiderling, *J. Am. Chem. Soc.* 127 (2005) 4992–4993.
- [22] T.A. Keiderling, in: N. Berova, K. Nakanishi, R.W. Woody (Eds.), *Circular Dichroism: Principles and Applications*, Wiley-VCH, New York, 2000, pp. 621–666.
- [23] T.A. Keiderling, *Curr. Opin. Chem. Biol.* 6 (2002) 682–688.
- [24] T.A. Keiderling, J. Kubelka, J. Hilario, in: M. Braiman, V. Gregoriou (Eds.), *Vibrational Spectroscopy of Polymers and Biological Systems*, Marcel–Dekker Publ, New York, 2005.
- [25] T.A. Keiderling, R.A.G.D. Silva, in: M. Goodman, G. Herrman (Eds.), *Synthesis of Peptides and Peptidomimetics*, Georg Thieme Verlag, Stuttgart, 2002, pp. 715–738.
- [26] R. Schweitzer-Stenner, G. Sieler, N.G. Mirkin, S. Krimm, *J. Phys. Chem.* 102 (1998) 118–127.
- [27] J.W. Brauner, C.R. Flack, R. Mendelsohn, *J. Am. Chem. Soc.* 127 (2005) 100–109.
- [28] J.W. Brauner, C. Dugan, R. Mendelsohn, *J. Am. Chem. Soc.* 122 (2000) 677–683.
- [29] J.H. Choi, M. Cho, *J. Chem. Phys.* 120 (2004) 4383–4392.
- [30] J.H. Choi, J.S. Kim, M. Cho, *J. Chem. Phys.* 122 (2005) 174903.
- [31] P. Bour, T.A. Keiderling, *J. Phys. Chem. B* 109 (2005) 5348–5357.
- [32] J. Kubelka, R. Huang, T.A. Keiderling, *J. Phys. Chem. B* 109 (2005) 8231–8243.
- [33] H. Fabian, D. Chapman, H.H. Mantsch, in: H.H. Mantsch, D. Chapman (Eds.), *Infrared Spectroscopy of Biomolecules*, Wiley–Liss, Chichester, 1996, pp. 341–52.
- [34] K. Halverson, I. Sucholeiki, T.T. Ashburn, P.T. Lansbury, *J. Am. Chem. Soc.* 113 (1991) 6701–6703.
- [35] S. Krimm, G. Zerbi (Eds.), *Modern Polymer Spectroscopy*, Wiley-VCH, 1999, pp. 239–85.
- [36] H. Torii, M. Tasumi, *J. Chem. Phys.* 96 (1992) 3379–3387.
- [37] P. Bour, J. Sopkova, L. Bednarova, P. Malon, T.A. Keiderling, *J. Comput. Chem.* 18 (1997) 646–659.
- [38] J. Kubelka, R.A.G.D. Silva, P. Bour, S.M. Decatur, T.A. Keiderling, in: J.M. Hicks (Ed.), *Chirality: Physical Chemistry*. ACS Symposium Series, American Chemical Society, Washington, DC, 2002, pp. 50–64.
- [39] J. Kubelka, T.A. Keiderling, *J. Am. Chem. Soc.* 123 (2001) 12048–12058.
- [40] J. Kubelka, T.A. Keiderling, *J. Am. Chem. Soc.* 123 (2001) 6142–6150.
- [41] H. Torii, M. Tasumi, *J. Raman Spectrosc.* 29 (1998) 81–86.
- [42] W.H. Moore, S. Krimm, *Proc. Natl. Acad. Sci. U.S.A.* 72 (1975) 4933–4935.
- [43] S. Krimm, J. Bandekar, *Adv. Protein Chem.* 38 (1986) 181–364.
- [44] S.H. Lee, S. Krimm, *Chem. Phys.* 230 (1998) 277–295.
- [45] P. Bour, Computational study of the vibrational optical activity of amides and peptides, Ph.D. Thesis, Academy of Science of the Czech Republic, Prague, Czech Republic, 1993.
- [46] P. Bour, J. Kubelka, T.A. Keiderling, *Biopolymers* 53 (2000) 380–395.
- [47] J. Kubelka, R.A.G.D. Silva, T.A. Keiderling, *J. Am. Chem. Soc.* 124 (2002) 5225–5232.
- [48] P. Bour, J. Kubelka, T.A. Keiderling, *Biopolymers* 65 (2002) 45–69.
- [49] J. Kubelka, IR and VCD spectroscopy of model peptides. Theory and experiment, Ph.D. thesis, University of Illinois at Chicago, Chicago, 2002.
- [50] R.D.B. Fraser, T.P. McRae, *Conformation in Fibrous Proteins*, Academic Press, New York, 1973.
- [51] M.J. Frisch, G.W. Trucks, H.B. Schlegel, G.E. Scuseria, M.A. Robb, J.R. Cheeseman, V.G. Zakrzewski, J. Montgomery, J.A.R.E. Stratmann, J.C. Burant, S. Dapprich, J.M. Millam, A.D. Daniels, K.N. Kudin, M.C. Strain, O. Farkas, J. Tomasi, V. Barone, M. Cossi, R. Cammi, B. Mennucci, C. Pomelli, C. Adamo, S. Clifford, J. Ochterski, G.A. Petersson, P.Y. Ayala, Q. Cui, K. Morokuma, D.K. Malick, A.D. Rabuck, K. Raghavachari, J.B. Foresman, J. Cioslowski, J.V. Ortiz, B.B. Stefanov, G. Liu, A. Liashenko, P. Piskorz, I. Komaromi, R. Gomperts, R.L. Martin, D.J. Fox, T. Keith, M.A. Al-Laham, C.Y. Peng, A. Nanayakkara, C. Gonzalez, M. Challacombe,

- P.M.W. Gill, B. Johnson, W. Chen, M.W. Wong, J.L. Andres, C. Gonzalez, M. Head-Gordon, E.S. Replogle, J.A. Pople, Gaussian 98, Gaussian Inc., Pittsburgh, PA, 1998
- [52] A. Becke, *Phys. Rev. A* 38 (1988) 3098–3100.
- [53] A.D. Becke, in: D.R. Yarkony (Ed.), *Modern Electronic Structure Theory*, World Scientific, Singapore, 1995, pp. 1022–1046.
- [54] J.P. Perdew, Y. Wang, *Phys. Rev. B* 45 (1992) 13244.
- [55] J.P. Perdew, Y. Wang, *Phys. Rev. B* 33 (1988) 8800–8802.
- [56] J. Kubelka, T.A. Keiderling, *J. Phys. Chem. A* 105 (2001) 10922–10928.
- [57] J.R. Cheeseman, M.J. Frisch, F.J. Devlin, P.J. Stephens, *Chem. Phys. Lett.* 252 (1996) 211–220.
- [58] P.J. Stephens, C.S. Ashvar, F.J. Devlin, J.R. Cheeseman, M.J. Frisch, *Mol. Phys.* 89 (1996) 579–594.
- [59] P.J. Stephens, F.J. Devlin, C.S. Ashvar, C.F. Chabalowski, M.J. Frisch, *Faraday Discuss.* 99 (1994) 103–119.
- [60] S. Krimm, W.C. Reisdorf Jr., *Faraday Discuss.* 99 (1994) 181–194.
- [61] P. Bour, T.A. Keiderling, *J. Am. Chem. Soc.* 114 (1992) 9100–9105.
- [62] J. Hilario, J. Kubelka, T.A. Keiderling, *J. Am. Chem. Soc.* 125 (2003) 7562–7574.
- [63] P.J. Stephens, *J. Phys. Chem.* 91 (1987) 1712–1715.
- [64] S. Krimm, in: B.R. Singh (Ed.), *Infrared Analysis of Peptides and Proteins: Principles and Applications*. ACS Symposium Series, ACS, Washington, DC, 2000, pp. 38–53.
- [65] Y.N. Chirgadze, N.A. Nevskaya, *Biopolymers* 15 (1976) 607–625.
- [66] T. Miyazawa, *J. Chem. Phys.* 32 (1960) 1647–1652.
- [67] P. Bour, T.A. Keiderling, *J. Phys. Chem. B* 109 (2005) 23687–23697.

Author's personal copy